Obelin from the Bioluminescent Marine Hydroid *Obelia geniculata*: Cloning, Expression, and Comparison of Some Properties with Those of Other Ca^{2+}-Regulated Photoproteins†

Svetlana V. Markova,‡,§ Eugene S. Vysotski,‡,§ John R. Blinks,|| Ludmila P. Burakova,‡ B-C. Wang,§ and John Lee*,§

Photobiology Laboratory, Institute of Biophysics, Russian Academy of Sciences, Siberian Branch, Krasnoyarsk 660036, Russia, Friday Harbor Laboratories, University of Washington, Friday Harbor, Washington 98250, and Department of Biochemistry and Molecular Biology, University of Georgia, Athens, Georgia 30602

Received September 13, 2001; Revised Manuscript Received December 13, 2001

ABSTRACT: A cDNA encoding the Ca^{2+}-regulated photoprotein of the bioluminescent marine hydroid *Obelia geniculata* was cloned and sequenced. The cDNA is a 774 bp fragment containing two overlapping open reading frames, one of which contained 585 bp encoding a 195 amino acid polypeptide which obviously has the primary structure of the apoprotein of a calcium-regulated photoprotein. Many of the residues are identical to those in other Ca^{2+}-regulated photoproteins: 86% compared with that from *Obelia longissima*, 76% with that from *Clytia* (*Phialidium*), 64% with that from *Aequorea*, and 64% with that from *Mitrocoma* (*Halistaura*). The obelin from *O. geniculata* was overexpressed in *Escherichia coli*, refolded from inclusion bodies, and purified. The yield of highly purified recombinant protein was 55−80 mg/L of LB medium. *O. geniculata* obelin has absorption maxima at 280 and 460 nm and a shoulder at approximately 310 nm. The calcium-discharged protein loses visible absorption but exhibits a new absorption maximum at 343 nm. The bioluminescence of the obelin from *O. geniculata* is blue (λ_{max} = 495 nm). In contrast, the fluorescence of the calcium-discharged protein is yellow-green (λ_{max} = 520 nm; excitation at 340 nm). This is in sharp contrast to aequorin in which the bioluminescence and fluorescence emission spectra of the calcium-discharged protein are almost identical (λ_{max} = 465 nm). The Ca^{2+} concentration−effect curve for *O. geniculata* obelin is similar to those of many other photoproteins: at [Ca^{2+}] below approximately 10^{-8} M, calcium-independent luminescence is observed, and at [Ca^{2+}] approximately 10^{-3} M, the luminescence reaches a maximum. Between these extremes, the curve spans a vertical range of almost 8 log units with a maximum slope on a log−log plot of about 2.5. In the absence of Mg^{2+} the rate constant for the rise of bioluminescence determined by the stopped-flow technique is about 450 s^{-1}. The effects of Mg^{2+} on the kinetics of bioluminescence are complicated, but at all concentrations studied they are relatively small compared to the corresponding effects on aequorin luminescence. At least with respect to speed and sensitivity to Mg^{2+}, the obelins from both *O. longissima* and *O. geniculata* would appear to be more suitable than aequorin for use as intracellular Ca^{2+} indicators.

The term "photoprotein" was introduced by Shimomura and Johnson (*1*) as a convenient, general designation for certain bioluminescent proteins that do not fit the classical concept according to which an enzyme (the luciferase) catalyzes the oxidation of a smaller organic substrate molecule (the luciferin) with the creation of an excited state and the emission of light. Thus, they defined a photoprotein as a protein that directly participates in the light-emitting reaction of a living organism, that is capable of emitting light in proportion to the amount of the protein (rather than in proportion to some substrate such as a luciferin), and that is not the unstable, transient intermediate of an enzyme−substrate reaction. Photoproteins such as aequorin do in fact hold a stabilized intermediate of the reaction pathway (*2*). Though other kinds of photoproteins have been described, the great majority of photoproteins now known to exist are stimulated to luminescence by calcium or certain other inorganic ions, and the term "calcium-activated photoproteins" was applied to them by Hastings and Morin (*3*). More recently, the term "calcium-regulated photoproteins" was suggested (*4*) to refer to this group, first because these proteins are members of the family of calcium-regulated effector proteins such as calmodulin and troponin C that play such an important role in controlling a variety of cellular functions and second because calcium regulates the function of these proteins but is not essential for it.

† This work was supported by ONR Grant N 00014-99-1-0414, Georgia Research Alliance, Grant 99-04-48452 from the Fundamental Research Foundation of the Russian Academy of Sciences, and Grant NA76RG0119, Project R/B-32, from the National Oceanic and Atmospheric Administration to Washington Sea Grant Program, University of Washington. The views expressed herein are those of the authors and do not necessarily reflect the views of NOAA or any of its subagencies.

* Author for correspondence. E-mail: jlee@arches.uga.edu. Tel: (706) 542-1764. Fax: (706) 542-1738.

‡ Russian Academy of Sciences.

§ University of Georgia.

|| University of Washington.

10.1021/bi0117910 CCC: $22.00
Published on Web 01/26/2002

Ca^{2+}-regulated photoproteins are found in and are responsible for the light emission of a variety of bioluminescent marine organisms, mostly coelenterates. The best known of these is aequorin, first isolated in 1962 by Shimomura et al. (*5*) from the jellyfish *Aequorea*. The Ca^{2+}-regulated photoproteins consist of a single polypeptide chain to which an imidazolopyrazinone derivative (called coelenterazine) is tightly bound. The light-yielding reaction proceeds at a very low rate in the absence of Ca^{2+} but is greatly accelerated when Ca^{2+} binds to the protein. The reaction is an oxidative decarboxylation of the coelenterazine, with the elimination of a mole of carbon dioxide and the generation of the protein-bound product (called coelenteramide) in an excited state (*6*, *7*).

Although Ca^{2+}-regulated photoproteins have apparently been detected in a great many (more than 25) different coelenterates (*8*), only six such proteins have so far been isolated in an even partially purified state. These are aequorin (*5*), halistaurin (mitrocomin) (*9*), and phialidin (clytin) (*10*) from the jellyfish *Aequorea*, *Halistaura* (*Mitrocoma*), and *Phialidium* (*Clytia*), respectively; obelin from the marine hydroids *Obelia geniculata* (*11*, *12*), *Obelia australis* (*12*), and *Obelia longissima* (*13*); and mnemiopsin and berovin (*14*, *15*) from the ctenophores *Mnemiopsis* and *Beroe*. During the past 15 years, cloning and sequence analysis have been achieved for cDNAs coding for four Ca^{2+}-regulated photoproteins: aequorin (*16*−*18*), phialidin (clytin) (*19*), halistaurin (mitrocomin) (*20*), and the obelin from *O. longissima* (*21*, *22*). All Ca^{2+}-regulated photoproteins show high sequence homology and contain three "EF-hand" calcium-binding sites (*22*−*24*). Apoproteins expressed by *Escherichia coli* can be charged to active photoproteins by incubating them with synthetic coelenterazine under calcium-free conditions in the presence of O_2 and β-mercaptoethanol or dithiothreitol.

Recently, the three-dimensional crystal structures have been solved for aequorin with resolution of 2.3 Å (*25*) and the obelin from *O. longissima* at 1.7 Å (*26*) and 1.1 Å (*27*). As expected from the homology of their primary sequences, both photoproteins have the same general tertiary structure, a compact globule containing four helix−turn−helix (HTH)[1] motifs, the second of which does not bind Ca^{2+}. The coelenterazine binding site in both structures is located in a corresponding position. In the aequorin structure two oxygen atoms were observed substituted at the C-2 position of the bound coelenterazine (*25*) in accordance with the predicted peroxide structure (*28*).

The main use of Ca^{2+}-regulated photoproteins has been for the detection of calcium ions in biological systems (*29*). Photoproteins have now been used successfully in a great many different types of living cells, both to estimate the intracellular [Ca^{2+}] under steady-state conditions and to study the role of calcium transients in the regulation of cellular function. Two photoproteins have been used in this way: aequorin and obelin. However, only aequorin has been used widely, perhaps partly because it was the first photoprotein to be discovered but more significantly because of its more general availability. Nonetheless, aequorin has a number of shortcomings that have limited its utility. Among the most important of these are that it responds too slowly to follow the most rapid intracellular calcium transients without distortion (*30*) and that physiological concentrations of magnesium antagonize the effects of calcium and slow the kinetics even further (*31*). Other Ca^{2+}-regulated photoproteins do not necessarily share these defects in equal measure. For example, obelin is considerably faster (*12*, *32*), and obelin (*32*) and halistaurin (*33*) are relatively insensitive to physiological concentrations of magnesium. Although aequorin's range of calcium sensitivity suits it well for the majority of applications, there are circumstances in which it would be useful to have photoproteins with higher or lower calcium sensitivity. Phialidin is apparently less sensitive (*34*), and it has been reported that the Ca^{2+} sensitivity of aequorin can be reduced deliberately by certain modifications in the Ca^{2+}-binding sites (*35*). There are, as yet, no reported examples of Ca^{2+}-regulated photoproteins with Ca^{2+} sensitivities significantly higher than those of aequorin or obelin, but they may yet be found. Presumably, differences in properties of the sorts under discussion originate from differences in primary sequences and tertiary structure among the photoproteins. Two approaches can be used to elucidate this structure/function relation: the properties of naturally occurring photoproteins with different sequences can be compared or new photoproteins can be created by site-directed mutagenesis. Sometimes, clues to productive avenues for mutagenesis can be derived from the comparison of photoproteins from different species or genera, most of which probably occur as multiple isoforms with minor differences in sequence, even within an individual organism.

Here we describe the cloning, expression, sequencing, and some properties of recombinant obelin from *O. geniculata* and compare those properties to those of obelin from *O. longissima*. Though the two varieties of obelin are very similar, there are some clear differences between them.

EXPERIMENTAL PROCEDURES

Reagents. The SMART cDNA Library Construction Kit was from Clontech (Palo Alto, CA), MMLV RNase H^- reverse transcriptase Superscript II was from Life Technology (Gaithersburg, MD); Gigapack III Gold packaging kit, cloned PfuTurbo polymerase, reagents for PCR, and competent cells of *E. coli* strains XL1-Blue and BL21-Gold, were from Stratagene (La Jolla, CA). Oligonucleotides were purchased from MWG-Biotech (High Point, NC). Restriction and modification enzymes were from Promega (Madison, WI). The Manual DNA Cycle Sequencing Kit was from Medigen (Novosibirsk, Russia). Coelenterazine was from Prolume Ltd. (Pittsburgh, PA). Chelex-100 chelating resin (100−200 mesh), Bio-Gel P2 resin, and the Bio-Scale DEAE 10 anion-exchange column were from Bio-Rad (Richmond, CA). DEAE-Sepharose Fast Flow was from Amersham-Pharmacia-Biotech (Piscataway, NJ). EGTA was from Fluka (batch number 276355/1 1291). All other chemicals were from standard sources and were of reagent grade or better.

[1] Abbreviations: HTH, helix−turn−helix; IPTG, isopropyl β-D-thiogalactopyranoside; DTT, DL-dithiothreitol; EDTA, ethylenediaminetetraacetic acid; EGTA, ethylene glycol bis(2-aminoethyl)-*N*,*N*,*N*′,*N*′-tetraacetic acid; PIPES, 1,4-piperazinebis(ethanesulfonic acid); *Ol*-obelin, recombinant obelin from *Obelia longissima*, the clone described in ref *29* (NCBI access number Q27709); *Og*-obelin, recombinant obelin from *Obelia geniculata*, the clone described in this paper (NCBI access number AF394688); L_{max}, the peak light intensity recorded when an aliquot of photoprotein is rapidly mixed with a saturating [Ca^{2+}]; L_{int}, the time integral of the light flash recorded when an aliquot of photoprotein is rapidly mixed with [Ca^{2+}].

Hydroid Collection. Colonies of *O. geniculata* were collected attached to fronds of the brown alga *Laminaria* in Chupa Bay of the White Sea, at the Marine Biological Station "Kartesh" of the Institute of Zoology, Russian Academy of Sciences. The living colonies were individually cut off the seaweed, drained on nylon mesh, placed into plastic tubes, and quickly frozen with liquid nitrogen. The colonies were stored in liquid nitrogen until required.

Preparation of the Expression cDNA Library and Screening. Total RNA was isolated from frozen whole *O. geniculata* colonies by means of the guanidine isothiocyanate−phenol method (*36*). Poly(A)+ RNA was purified on poly(U)− Sepharose 4B (Pharmacia), and 1 μg of this was employed to synthesize cDNA. The expression cDNA library was constructed with the SMART cDNA Library Construction Kit according to the protocol supplied with the kit, in a λTriplEx2 phagemid vector. The cDNA-vector ligation mixture obtained was then packaged with Gigapack II Gold packaging extract, yielding about 10^6 independent recombinant plaques. The phage and bacterial culture plating was carried out according to the protocol for the SMART cDNA Library Construction Kit. For screening the unamplified phage a cDNA library was plated at low density. An imprint of the plaque pattern was obtained by applying a dry nitrocellulose filter impregnated with bacteria to the primary plate. The filter was then turned over, applied to a fresh sterile agar plate, and left on the plate for the bacteria to grow. The replica filters were grown until a bacterial lawn with clearly visible plaques appeared. Then the bacterial lawn with plaques was scraped off the filter with a sterile glass spreader into LB medium supplemented with 10 mM $MgSO_4$ and 0.2% maltose. The suspension was poured into a culture tube, and gene expression was induced with 20 μM IPTG for 1 h at 37 °C. The cell pellet from 3 mL of suspension was sonicated in 0.3 mL of 5 mM EDTA and 20 mM Tris-HCl, pH 7.0 at 0 °C. The crude cell lysate was charged with coelenterazine (final concentration 10^{-7} M) in the presence of 10 mM DTT and assayed for bioluminescence activity. The next replica from a positive primary plate was cut into sectors for a more detailed location of positive plaques and was analyzed as above. Then the individual plaques from the positive areas were isolated and assayed for bioluminescence activity after IPTG induction. The isolated cDNA was cycle-sequenced according to the protocol supplied with the Manual DNA Cycle Sequencing Kit. [α-^{32}P]dATP was used as a label.

Sequence Analysis. The computer program ClustalW 1.81 was used for sequence comparison and alignment.

Expression of Recombinant O. geniculata obelin in E. coli. The coding sequence for *O. geniculata* obelin was amplified by PCR: the plasmid with the cloned *O. geniculata* cDNA gene was used as a template with a forward primer containing a *Nco*I site and a reverse primer containing a *Xho*I site. Primers used were forward 5′-ACTCCATTGCTTCCAAATACGCAGT-3′ and reverse 5′-ACTCTGCAGTTTAGGGGACTCCATTTCCG-3′. The PCR reaction was carried out in 50 μL of 1× PfuTurbo buffer with 100 pmol of primers, 250 μM each dNTP, 100 ng of the cDNA, and 2.5 units of cloned PfuTurbo polymerase (Stratagene) for 12 cycles. Each cycle consisted of 20 s at 94 °C, 30 s at 55 °C, and 30 s at 72 °C, with a final extension of 2 min. The PCR product was digested with *Nco*I and *Xho*I and gel-purified. Then the restricted product was inserted in-frame into the *Nco*I/*Xho*I sites of the expression vector pET19b (Novagen, Madison, WI) immediately behind the initiator methionine codon and transformed into XL1Blue competent bacterial cells for sequence analysis. The resulting plasmid was named pET19-OG. After verification of the nucleotide sequence, the pET19-OG was introduced into *E. coli* strain BL21(DE3)-Gold for expression of *O. geniculata* apoobelin.

Growth of Bacterial Cultures and Induction. E. coli BL21-(DE3)-Gold cells were grown in media containing 200 μg/mL ampicillin or 50 μg/mL carbenicillin. For protein production, the transformed *E. coli* BL21-Gold was cultivated with vigorous shaking at 37 °C in LB medium containing ampicillin and induced with 1 mM IPTG when the culture reached an OD_{600} of 0.5−0.6. After addition of IPTG, the cultivation was continued for 3 h.

Bioluminescence Assay. The bioluminescence was measured with a custom-made photometer or a Turner TD-20e luminometer by rapid injection of 10 μL of the photoprotein sample or 100 μL of charged crude cell lysate into a luminometer cell containing 1 mL of a solution of 100 mM $CaCl_2$ and 100 mM Tris-HCl, pH 7.0, at room temperature.

Spectral Measurements. Absorption spectra were obtained with a Hewlett-Packard 8453 UV−visible spectrophotometer and bioluminescence and fluorescence spectra with an SLM-8000 spectrofluorometer. Emission spectra were corrected by reference to the absolute fluorescence spectral distribution of quinine sulfate, which was also used as the reference for the fluorescence quantum yield. The excitation spectra were corrected for spectral variations from the excitation source by reference to a rhodamine-B quantum counter. The bioluminescence reaction was at 20 °C from obelin in 1 mM EDTA and 10 mM Tris-HCl, pH 7.0, and was initiated by injection of $CaCl_2$. The final concentration of free calcium was 0.5 μM in order to provide a constant light level during the spectral scan. The amount of $CaCl_2$ to be added was calculated with the MAXCHELATOR program.

Ca^{2+} Concentration−Effect Curves and Rapid-Mixing Kinetic Measurements. These measurements were carried out with EDTA-free solutions of obelin. EDTA was removed from the purified photoprotein by gel filtration on a 0.9 × 25 cm bed of Bio-Gel P6 in a Pharmacia K9/30 plastic column. The column was equilibrated and eluted with 150 mM KCl and 5 mM PIPES, pH 7.0, which had been previously passed (three times) through freshly washed beds of Chelex-100 chelating resin (for details of preparing Chelex, see ref *37*). The fractions containing photoprotein were identified by luminescence assay. To avoid possible contamination with EDTA, only the first few photoprotein fractions to come off the column were used for the determination of Ca^{2+} concentration−effect curves and for kinetic measurements.

Ca-EGTA buffers (total [EGTA] = 2 mM) were used to establish Ca^{2+} concentrations below about 10^{-5} M and simple dilutions of $CaCl_2$ (in a Chelex-scrubbed solution of 150 mM KCl and 5 mM PIPES, pH 7.0) for higher Ca^{2+} concentrations. The Ca^{2+} buffers were prepared by the two stock solution method and corrected as described by Klabusay and Blinks (*38*). When high concentrations of Ca^{2+} or Mg^{2+} were added, [KCl] was reduced to keep the ionic strength constant. When measurements were to be made in solutions containing Mg^{2+}, the obelin was preequilibrated with the same [Mg^{2+}].

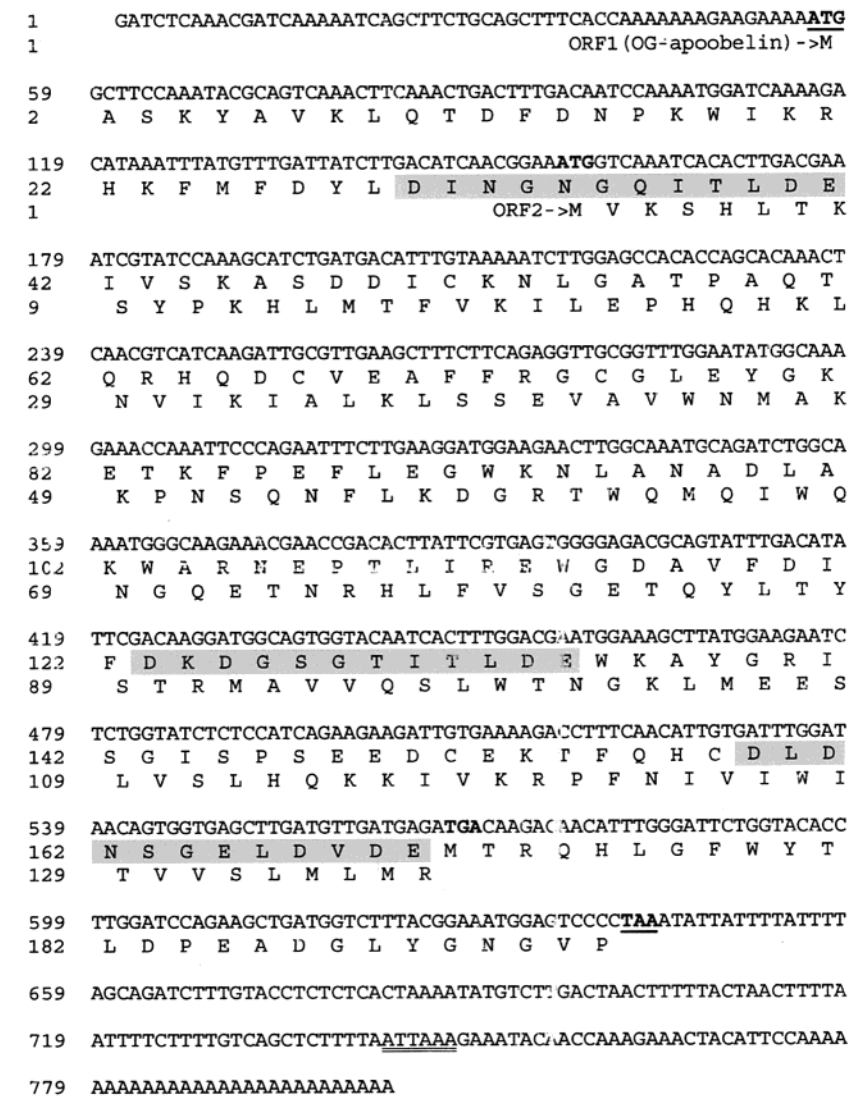

FIGURE 1: Nucleotide sequence of the cDNA for *O. geniculata* obelin and deduced amino acid sequences of two open reading frames (ORF1 for *O. geniculata* apoobelin and ORF2). The translation signals within the sequence are in bold. The polyadenylation signal, ATTAAA, is underlined. Ca^{2+}-binding sites of *O. geniculata* obelin are denoted by the light gray boxes.

For the Ca^{2+} concentration−effect curves, peak light intensity was measured after 10 μL of the photoprotein solution was forcefully injected into 1 mL of the test solution, as previously described (*39*). Light intensity (L) measurements were converted to units of L/L_{int} by first calculating L/L_{max} and then multiplying by the maximum peak-to-integral ratio (L_{max}/L_{int}) determined from stopped-flow measurements carried out under the same conditions and with the same sample of obelin. The kinetics of the light response after sudden exposure to a saturating Ca^{2+} concentration were examined with an air-driven adaptation of the stopped-flow machine described by Gibson and Milnes (*40*). For these experiments it was fitted with a single mixer in order to minimize the deadtime, which with the air pressure used was 1.5−2.0 ms. Light was gathered and conducted from the reaction tube to an EMI 9635 photomultiplier by three fiber-optic probes applied around the circumference of the tube at a point approximately 25 mm downstream from the mixer.

The signal from the photomultiplier was recorded through an operational amplifier wired as current-to-voltage converter with a time constant of 0.1 ms, and signals were captured with a Nicolet Model 4094C digital oscilloscope operating in the pretriggered mode with digital sampling at 0.01−1 ms intervals. To reduce photomultiplier shot noise, several successive signals (usually 5 or 10) were averaged.

RESULTS AND DISCUSSION

Isolation of a Positive Clone, cDNA Structure, and Sequence. The *O. geniculata* cDNA library yielded approximately 10^6 independent recombinant plaques. After about 30000 plaques had been screened, one positive clone with luminescence activity was isolated. The isolated cDNA (NCBI access number AF394688) is a 774 bp fragment with a 55 bp 5′ untranslated region upstream from the first start codon (Figure 1). One open reading frame (ORF1) contains 585 bp, which encodes a 195 amino acid polypeptide (Figure 1) homologous with the photoprotein family. After the stop codon there is a 131 bp untranslated region followed by a terminal 28 bp poly(A) tail. Additionally, there is a second long open reading frame (ORF2) within the same cDNA sequence of the photoprotein, extending from bp 156 to 569 (Figure 1). This ORF2 in the cloned cDNA consists of 137 codons and encodes a 16.1 kDa alkaline polypeptide of unknown function (predicted isoelectric point 10.9). It is

```
OG-obelin      1 ---MASKYAVKLQTDFDNPKWIKRHKFMFDYLDINGNGQITLDEIVSKAS
OL-obelin      1 ---.S.......K......R......H...F.......K.............
Clytin         1 MADT........RPN......VN......NF.....D.K.............
Aequorin       1 --MTSKQ.S...TS.....R..G...H..NF..V.H..K.S...M.Y...
Mitrocomin     1 -MS.G.R.....T.........A...H..NF....S....N.N.M.H...
                                                    I

OG-obelin     48 DDICKNLGATPAQTQRHQDCVEAFFRGCGLEYGKETKFPEFLEGWKNLAN
OL-obelin     48 ....AK.E...E..K...V..........M.....IA..Q..D...Q..T
Clytin        51 ....AK.....E..K....A.....KKI.MD....VE..A.VD...E...
Aequorin      49 .IVIN......E.AK..K.A.....G.A.MK..V..DW.AYI....K..T
Mitrocomin    50 NI...K....EE..K...K...D..G.A....D.D.TW..YI....R..K

OG-obelin     98 ADLAKWARNEPTLIREWGDAVFDIFDKDGSGTITLDEWKAYGRISGISPS
OL-obelin     98 SE.K.....................................K.......
Clytin       101 Y..KL.SQ.KKS...D..E.............S.S.............CS.
Aequorin      99 DE.E.Y.K.......I....L...V...QN.A.........TKAA..IQ.
Mitrocomin   100 TE.ERHSK.QV....L....L...I...RN.SVS....IQ.THCA..QQ.
                                                  II

OG-obelin    148 EEDCEKTFQHCDLDNSGELDVDEMTRQHLFWYTLDPEADGLYGNGVP-
OL-obelin    148 Q....A..R.......D.........................-
Clytin       151 D..A....K.......K.................N.......F..-
Aequorin     149 S....E..RV..I.E..Q...............M..ACEK...GA..-
Mitrocomin   150 RGQ..A..A....GD.K.....  .........SV..TCE....GA..Y
                          III
```

FIGURE 2: Comparison of the primary structure of obelin from *O. geniculata* (OG) with those of four other photoproteins: *O. longissima* obelin (OL) (*21*), aequorin AQ440 (*16*), phialidin (clytin) (*18*), and halistaurin (mitrocomin) (*19*). Dots indicate the sequence positions in which the amino acid residue matches that in the sequence for *O. geniculata* obelin. Gaps are shown by dashes. Ca^{2+}-binding sites (I, II, and III) of photoproteins are denoted by the shaded boxes.

interesting that a similar internal ORF2 (though longer by two codons) was found within the cDNA sequence of *O. longissima* obelin (*22*) but not in those for aequorin, clytin, or mitrocomin.

As expected, the primary structure of *O. geniculata* obelin is very similar to that of other photoproteins. Like *O. longissima* obelin, clytin, and aequorin, *O. geniculata* obelin has three Ca^{2+}-binding sites and Pro at the C-terminus. The overall degree of identity between the amino acid sequence of *O. geniculata* obelin and the sequences of *O. longissima* obelin, clytin (phialidin), aequorin, and mitrocomin (halistaurin) is 86%, 76%, 64%, and 64%, respectively. The amino acid sequence of *O. geniculata* obelin differs from that of *O. longissima* obelin in 27 positions. However, the degree of identity of *O. geniculata* obelin with some other calcium-binding proteins, for example, sarcoplasmic calcium-binding protein (*41*), caltractin (*42*), calmodulin (*43*), troponin C (*44*), and calmodulin from *Renilla* (*45*), is significantly low, not more than 25%. Interestingly, the degree of identity between *O. geniculata* obelin and the calcium-dependent coelenterazine-binding protein from *Renilla* (*46*) is only 16%.

The degree of identity of the 12 amino acid residues forming the Ca^{2+}-binding sites (Figure 2, shaded boxes) was also calculated. Between *O. geniculata* obelin and *O. longissima* obelin, clytin, aequorin, and mitrocomin, respectively, it is as follows: for Ca^{2+}-binding site I, 91%, 83%, 66%, and 75%; for Ca^{2+}-binding site II, 100%, 83%, 75%, and 58%; for Ca^{2+}-binding site III, 91%, 91%, 75%, and 75%. Between the two obelins there is a difference of one residue in the seventh position of each of two Ca^{2+}-binding loops (I and III). The general similarity of the properties of the two photoproteins would suggest that the residues in question are not critically important to calcium binding.

Obelin Expression and Purification. As judged by SDS−PAGE analysis of the whole cell lysates (Figure 3), the yield

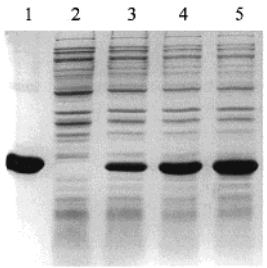

FIGURE 3: SDS−PAGE analysis of pET19-OG expression in *E. coli* BL21-Gold cells and obelin purity at the final step of purification. Lanes: 1, pooled activity peak from the last step of chromatography on a Bio-Scale DEAE 10 column; 2, whole cell lysate of *E. coli* cells before IPTG addition; 3−5, whole cell lysates of *E. coli* cells 1, 2, and 3 h after addition of IPTG. 12.5% polyacrylamide gels were stained with Coomassie blue.

of recombinant apoobelin obtained in *E. coli* BL21-Gold cells transformed with the pET19-OG plasmid is very high. The total amount of apoobelin increases during the first 3 h after addition of IPTG (Figure 3, lanes 3−5) and constitutes more than 50% of all cell protein. Further increasing the growing time after addition of IPTG does not produce a larger amount of protein (not shown). Most of the *O. geniculata* apoobelin produced is accumulated inside cells in inclusion bodies which can easily be isolated by centrifugation to yield highly concentrated and relatively pure protein.

The recombinant *O. geniculata* obelin was purified as previously reported for *O. longissima* protein (*32*) with some modifications. The apoobelin obtained after extraction with 6 M urea and through the first step of purification on a DEAE-Sepharose Fast Flow column was concentrated by ultrafiltration in an Amicon cell (YM10 membrane) to a final volume of 5−6 mL. To fold and charge the protein, the concentrated protein sample containing 6 M urea was diluted 20-fold with a solution containing 5 mM EDTA, 10 mM

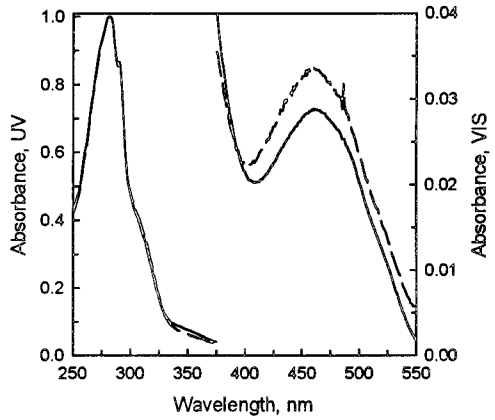

FIGURE 4: Absorption spectra of recombinant obelins from *O. longissima* (solid line) and *O. geniculata* (dashed line).

DTT, 20 mM Tris-HCl, pH 7.0, and coelenterazine (approximately 1 mol/mol of apoprotein) and incubated overnight at 4 °C. The final concentration of urea in the protein sample after dilution was approximately 0.3 M. The charged protein was then additionally purified on a Bio-Scale DEAE 10 anion-exchange column equilibrated with 5 mM EDTA and 20 mM Tris-HCl, pH 7.0. The obelin was eluted with a linear salt gradient of NaCl from 0 to 0.35 M at 2 mL/min. This chromatography step allows separation of the obelin from apoprotein that has not been charged with coelenterazine. The final product is homogeneous according to SDS−PAGE (Figure 3, lane 1) and LC-electrospray ionization mass spectrometry. The N-terminal amino acid sequence of the obelin showed that the first methionine is digested during production of the recombinant apoobelin in *E. coli* cells. The molecular mass of *O. geniculata* obelin determined by electrospray ionization mass spectrometry is in excellent agreement (to within 2 Da) with that calculated from the amino acid sequence. The yield of high-purity obelin ranges from 55 to 80 mg/L of LB medium depending on growth conditions. This recombinant obelin was used to produce high-quality crystals for structure determination by X-ray crystallography.

Spectral Properties. Figure 4 compares the absorption spectra of the two obelins. They both have absorption maxima at 280 and 460 nm and a shoulder at approximately 310 nm. The calcium-discharged obelins have essentially no absorption in the visible range but exhibit a new absorption maximum at 343 nm. Similar spectral results are observed for native aequorin and its calcium-discharged product (*47*).

The bioluminescence and fluorescence emission spectra of the Ca^{2+}-discharged obelins are shown in Figure 5. The bioluminescence spectral maximum for *O. geniculata* obelin is at 495 nm and for *O. longissima* obelin at 485 nm. These maxima are significantly different from that of aequorin (465 nm) and from both species of native obelins (475 nm) (*48*).

The binding of calcium to a photoprotein triggers oxidative decarboxylation of the coelenterazine to yield the bioluminescence emission, CO_2, and the oxidation product (coelenteramide) noncovalently bound to the apoprotein (*49*, *50*). Unlike the unreacted photoprotein the product is efficiently fluorescent, and in the case of aequorin, the uncorrected excitation maximum is 360 nm and the fluorescence spectrum has a $\lambda_{max} = 465$ nm with a spectral distribution similar to that of the bioluminescence. This aequorin product was therefore named "blue-fluorescent protein" (BFP), and this fluorescence property constitutes part of the identification of the excited state of this fluorophore as the directly formed product of the coelenterazine chemistry. In the case of aequorin, the BFP can be dissociated into apoprotein and coelenteramide by gel filtration in the presence of EDTA to remove the calcium (*49*). In contrast, the Ca^{2+}-discharged obelins, which both have an excitation peak at 340 nm, show a yellow-green (*O. geniculata*, $\lambda_{max} = 520$ nm) or green (*O. longissima*, $\lambda_{max} = 510$ nm) fluorescence (Figure 5). As the abbreviation "GFP" is widely used for another very famous protein also derived from a hydromedusan, we prefer to use the name "Ca^{2+}-discharged photoprotein" for these species.

Fluorescence studies of coelenteramide and its analogues in various solvents show that the coelenteramide can form five kinds of light emitters: the neutral species ($\lambda_{max} = 386-423$ nm), the phenolate anion ($\lambda_{max} = 480-490$ nm), an ion pair state ($\lambda_{max} = 465-479$ nm), the amide anion ($\lambda_{max} = 435-458$ nm), and a pyrazine N(4) anion ($\lambda_{max} = 530-565$ nm) (*51*). These model studies allow us to rationalize the spectral observations on the obelins. The bioluminescence spectra correspond more closely to the phenolate fluorescence than to the amide anion, the supposed primary species in the aequorin reaction. NMR evidence shows that a conformational change occurs on going to the Ca^{2+}-discharged *O. longissima* obelin (*52*). This change would be expected to

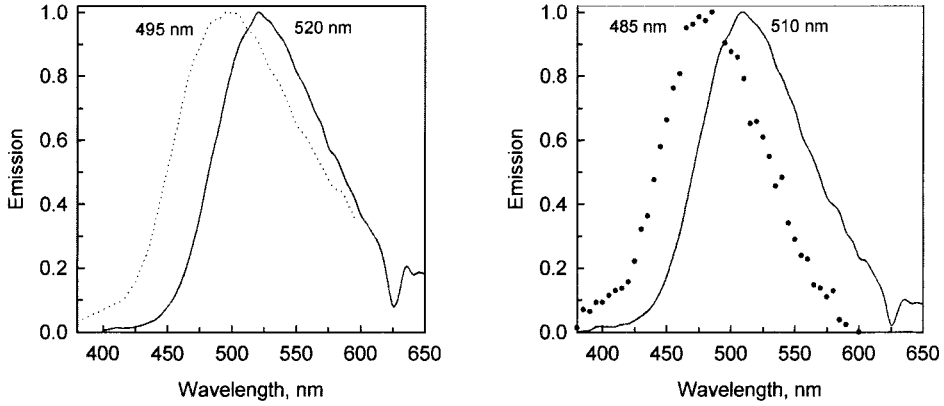

FIGURE 5: Comparison of the bioluminescence spectrum (dots) of each obelin with the fluorescence emission spectrum (line) of the corresponding Ca^{2+}-discharged obelin: left panel, recombinant obelin from *O. geniculata*; right panel, recombinant obelin from *O. longissima*. Wavelengths of spectral maxima are indicated.

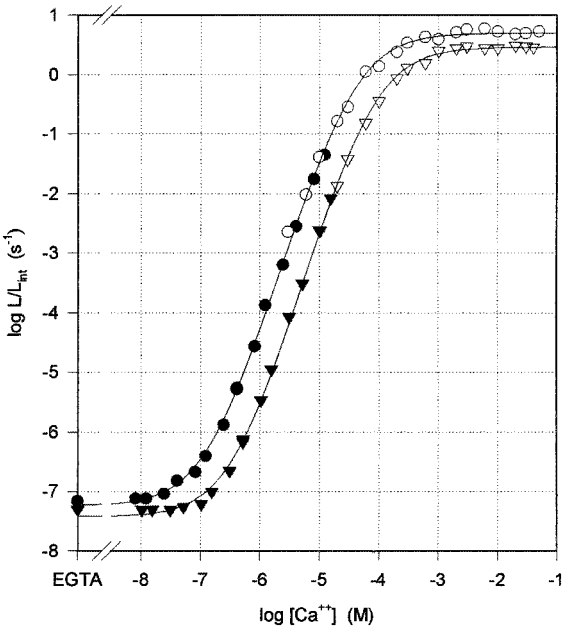

FIGURE 6: Ca^{2+} concentration−effect curves for recombinant *O. geniculata* obelin without (circles) and with (triangles) 10 mM Mg^{2+}, 20 °C. Symbols: filled, Ca-EGTA buffers; open, dilutions of $CaCl_2$. The curves were computer-fitted to the experimental points with the two-state model of Allen et al. (*54*) modified for use with light intensities expressed in terms of L/L_{int}.

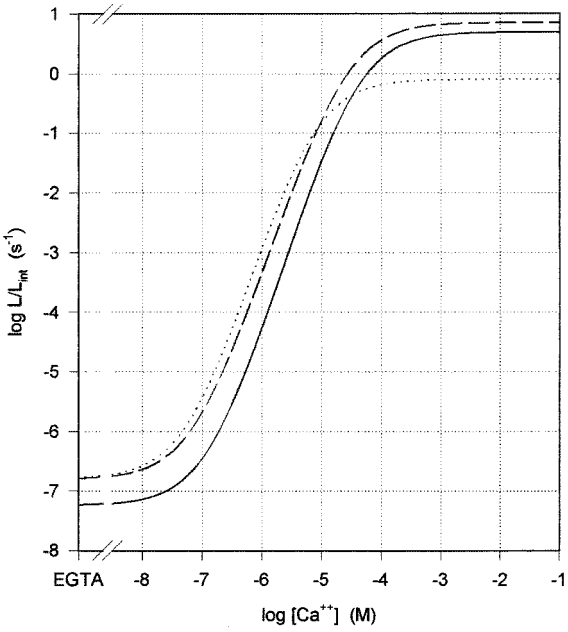

FIGURE 7: Ca^{2+} concentration−effect curve (20 °C) for obelin from *O. geniculata* (solid line) compared with those for *O. longissima* (dashed line) and for aequorin (clone AQ 440) (dotted line). The results for *Og*-obelin are from Figure 6; those for *Ol*-obelin and AQ 440 are from ref *32*. The curves were computer-fitted to the experimental points with the two-state model of Allen et al. (*54*) modified for use with light intensities expressed in terms of L/L_{int}.

be a slow process, and the final binding site environment of the product could well be different from that of the excited coelenteramide initially formed by the bioluminescence process. This explains why the fluorescence spectrum of the Ca^{2+}-discharged photoprotein is shifted to a longer wavelength from the bioluminescence, more closely resembling the model pyrazine N(4) anion fluorescence spectrum.

Calcium Concentration−Effect Relation. Figure 6 shows Ca^{2+} concentration−effect curves for the recombinant photoprotein from *O. geniculata* determined in the absence and presence of 10 mM Mg^{2+}. The curves are log−log plots in which light intensities have been expressed in terms of a ratio that we have termed the fractional rate of discharge (L/L_{int}) (*32*). This requires explanation, as it represents a departure from previous practice, in which light intensities have commonly been expressed in terms of the ratio L/L_{max}, where L is the peak light intensity measured from a sample of photoprotein when it is mixed with a Ca^{2+}-containing solution under a particular set of circumstances and L_{max} is the peak light intensity recorded from an identical sample when it is rapidly mixed with a saturating [Ca^{2+}] under the same conditions. Both measurements are expressed in the same units, so L/L_{max} is a dimensionless ratio. In the new expression, L has the same meaning as before, and L_{int} is the total amount of light emitted as the sample is discharged by Ca^{2+} (the time integral of the flash). Since L has units of photons per second and L_{int} is measured in photons, the ratio L/L_{int} has units of s^{-1}. While the expression has the units of a rate constant, nothing need be assumed about the time course of the flash. The light intensity measured at any instant is expressed as a fraction of the total amount of light that the sample is capable of emitting: hence the term "fractional rate of discharge". We find that L/L_{int} is a more useful and meaningful unit than L/L_{max}. Both units have the effect of normalizing the measurements for photoprotein concentration and for the optical efficiency of the measuring system, but L/L_{max} tends to obscure certain potentially significant characteristics of the light signal, such as the maximum peak-to-integral ratio, which can differ substantially from one photoprotein to the next, and is useful in the characterization of photoproteins. Another serious drawback of expressing light intensities in terms of L/L_{max} is that sometimes (as in the case of photoprotein mutants with reduced Ca^{2+} sensitivity) L_{max} cannot be measured meaningfully because it is not feasible to reach a saturating [Ca^{2+}] (without, for example, greatly increasing the ionic strength). If one assumes that quantum yield is constant, one can measure L_{int} without reaching L_{max} (for further discussion, see ref *32*). The Ca^{2+} concentration−effect curves for the recombinant photoprotein from *O. geniculata* (*Og*-obelin) in Figure 6 are similar to those published previously for that from *O. longissima* (*Ol*-obelin; Figure 7 and ref *32*), though there are distinct differences between them. (Whether these differences are greater than might be encountered among the products of different cDNA clones isolated from the same species remains to be seen.)

The peak-to-integral ratio in saturating [Ca^{2+}] is somewhat lower for *Og*-obelin (5.8) than for *Ol*-obelin (8.1), and partly as a result of this, the curve for *Og*-obelin lies below and somewhat to the right of that for *Ol*-obelin throughout its course (see Figure 7). In other words, for any given [Ca^{2+}], the light intensity and fractional rate of photoprotein consumption are somewhat higher for the obelin from *O. longissima* than for that from *O. geniculata.* Although the differences are not large, this should give the obelin from *O. longissima* a somewhat higher signal-to-noise ratio when the photoproteins are used as Ca^{2+} indicators. Other factors being equal, however, one might expect the obelin from *O. geniculata* to be a little more stable than that from *O. longissima*. At [Ca^{2+}] below approximately 10^{-8} M, both

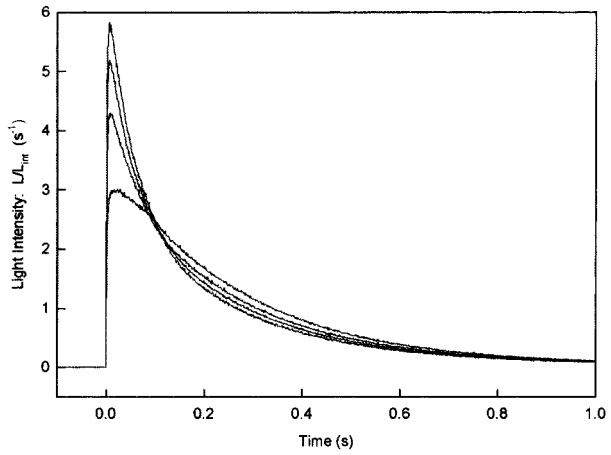

FIGURE 8: Influence of Mg^{2+} on the time course of the flash resulting from rapid mixing of *O. geniculata* obelin with Ca^{2+}. Stopped-flow records: final $[Ca^{2+}] = 20$ mM; 20 °C. Each trace is the product of averaging five sweeps. From the top: 0, 1, 3, and 10 mM Mg^{2+}.

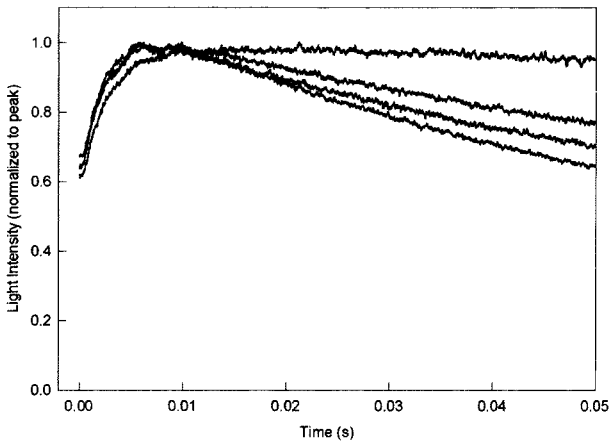

FIGURE 9: Effect of Mg^{2+} on the rate of rise of light intensity from *O. geniculata* obelin after rapid mixing with Ca^{2+}. Stopped-flow records: final $[Ca^{2+}] = 20$ mM; 20 °C. Each trace is the product of averaging of five sweeps. $Mg^{2+} = 0$, 1, 3, and 10 mM (slowest rise).

obelins have a low Ca^{2+}-independent luminescence and both rise to saturation at $[Ca^{2+}]$ approximately 10^{-3} M. Between these extremes, the curves span vertical ranges of approximately 8 log units with a maximum slope of about 2.5. This is somewhat greater than the span of the curve for aequorin (Figure 7), primarily because the maximum level of luminescence (expressed in terms of L/L_{int}) is nearly an order of magnitude higher for the obelins than for aequorin. (In other words, the peak-to-integral ratio in saturating $[Ca^{2+}]$ is higher for the obelins than for aequorin, which means of course that in saturating $[Ca^{2+}]$ the obelins will be discharged more rapidly than aequorin.) Below about 10^{-5} M Ca^{2+} the calcium sensitivity of the obelin from *O. longissima* is practically identical to that for recombinant aequorin from clone AQ440 (see Figure 7) (*17*, *32*).

The effects of Mg^{2+} on both obelins are much less pronounced than on aequorin, for which Mg^{2+} concentrations as low as 1 mM produce obvious decreases in the $[Ca^{2+}]$-independent luminescence, and the effects of 10 mM Mg^{2+} are substantial (*32*). Concentrations of Mg^{2+} that might be encountered inside living cells [in the vicinity of 1 mM (*53*)] have very little effect on the $[Ca^{2+}]$-independent luminescence or the Ca^{2+} sensitivity of either of the two obelins. Though slight, the effects of 10 mM Mg^{2+} on the Ca^{2+}-independent luminescence of the obelins from the two species are not the same. Whereas 10 mM Mg^{2+} has very little effect on the calcium-independent luminescence of the obelin from *O. longissima* (*32*) (and sometimes increases it slightly), it clearly decreases that of the obelin from *O. geniculata*. This was evident both from the curves of Figure 6 and from experiments in which Mg^{2+} was added directly to cuvettes containing EGTA and obelin.

Other effects of Mg^{2+} on the luminescence of the obelins are more obvious. Magnesium ions produce a decrease in the maximum level of luminescence attainable under the influence of Ca^{2+}, and this effect cannot be surmounted by increases in $[Ca^{2+}]$ (Figure 6 and ref *32*). (Note that the effect of Mg^{2+} appears more striking in the stopped-flow records of Figure 8 than in the Ca^{2+} concentration−effect curves of Figure 6, because the concentration−effect curves are plotted on a logarithmic scale.) Figure 6 also shows that 10 mM Mg^{2+} produced a modest rightward shift of the Ca^{2+} concentration−effect curve for the obelin from *O. geniculata*. This is similar to that for the obelin from *O. longissima* but much less pronounced than that for aequorin (*29*, *32*).

A Ca^{2+} concentration−effect curve for native obelin was published some time ago by Stephenson and Sutherland (*12*). The most striking difference between that curve and the ones shown in Figures 6 and 7 lies in the vertical span of the curves, which is barely more than 6 log units in the curve for native obelin and nearly 8 log units for the curves shown in Figures 6 and 7. A number of possible explanations come to mind: differences in photometer calibration, contamination of the solutions used in ref *12* with silver ions (likely source: pH reference electrode; see ref *29*), and species-to-species variation in the characteristics of the photoproteins studied. In contrast to the recombinant obelins used here, the native photoproteins were presumably heterogeneous mixtures of numerous isoforms. This is true of most (probably all) native photoproteins, but an additional complication is that Stephenson and Sutherland extracted their obelin from two different species of *Obelia*, *O. geniculata* and *O. australis*, and apparently used the products interchangeably. The source of the material used in the determination of the published Ca^{2+} concentration−effect curve was not stated (*12*).

Rapid-Mixing Stopped-Flow Kinetics. The speed with which the bioluminescence reaction responds to sudden changes in calcium concentration is of interest for both theoretical and practical reasons. From the theoretical standpoint, this information may allow inferences to be drawn about the chemistry of the reaction mechanism, notably the speed of the rate-limiting step in a putative reaction scheme. From the practical standpoint, the speed with which luminescence tracks rapid changes in $[Ca^{2+}]$ is important to the use of photoproteins as biological calcium indicators. Some photoproteins, notably aequorin (*12*, *30*, *32*), respond too slowly to follow rapid intracellular Ca^{2+} transients without distortion, and it would be useful to have faster ones.

Figures 8 and 9 show stopped-flow records for recombinant obelin from *O. geniculata* rapidly mixed with saturating $[Ca^{2+}]$ in the presence of various concentrations of Mg^{2+}. The slow sweep-speed records of Figure 8 show the full time course of the flash, while the higher speed tracings of Figure

9 are designed to show the rising phase, the speed of which limits the ability of the photoprotein to track very rapid Ca^{2+} transients. The light signals in Figure 8 are expressed in terms of fractional rate of discharge (L/L_{int}) to allow comparison of their amplitudes and time courses in absolute terms. In the high-speed tracings of Figure 9, each curve has been normalized to its own maximum in order to facilitate comparison of the rising phases. The same concentration of Mg^{2+} was added to both syringes of the stopped-flow machine to ensure that the photoprotein was always preequilibrated with the concentration of Mg^{2+} that was to be present in the solution after mixing. This is important because Mg^{2+} binds to the photoprotein much more slowly than does Ca^{2+}, and the effects of Mg^{2+} are attenuated if preequilibration is not achieved (*31*).

Figure 8 shows that the amplitude of the light signal induced by mixing *Og*-obelin with a saturating [Ca^{2+}] is substantially reduced by Mg^{2+}, even by Mg^{2+} concentrations as low as 1 mM. At the same time, the decay of the luminescence is slowed enough so that the total amount of light emitted in the flash is essentially unchanged. These tracings are very similar to comparable ones previously obtained with recombinant obelin from *O. longissima* (*32*).

From the practical standpoint the most important kinetic feature of the luminescence response of photoproteins is the rate of rise of light intensity after rapid mixing with Ca^{2+}: this is what limits the ability of the light signal to follow rapid changes in [Ca^{2+}]. Figure 9 shows that 1 and 3 mM Mg^{2+} had very little effect on the rate of rise of the light signal of *Og*-obelin, whereas 10 mM Mg^{2+} slowed it appreciably. This is similar to the result obtained with the obelin from *O. longissima*. However, rate constants for the rising phase (calculated by computer-fitting a single exponential to the experimental records) were slightly higher than those previously reported for *Ol*-obelin (446 vs 405 s^{-1} in the absence of Mg^{2+} and 405 vs 331 s^{-1} in 10 mM Mg^{2+}). The rates of rise that we have observed for both recombinant obelins are nearly twice those reported by Stephenson and Sutherland for native obelin (*12*). The difference probably results mainly from differences in instrumentation, as the results published in ref *12* were not obtained in a stopped-flow machine but in a mechanically stirred reaction cuvette in which mixing speed seems likely to have been limiting. Indeed, one may question the extent to which the rates of rise that we report here may have been slowed by inadequate mixing. Certainly we can readily distinguish between the rate constants for aequorin (115 s^{-1}) and obelin (at least 450 s^{-1}), but the higher rate constant should probably be regarded as a lower limit and subject to instrumental error. A separate issue is the fact that we are close to the limit imposed by the dead time of our stopped-flow machine. With a 1.5 ms dead time, 500 s^{-1} is about the highest first-order reaction rate that one can study and still have something to measure after flow stops (*40*).

For use as intracellular Ca^{2+} indicators, the obelins have two advantages over aequorin: they respond more rapidly, and they are less susceptible to interference by Mg^{2+}. This interference takes two forms: (1) Mg^{2+} reduces the speed with which a photoprotein can respond, and (2) it influences the position of the Ca^{2+} concentration−effect curve, which in the case of aequorin makes it necessary to know the intracellular [Mg^{2+}] in order to use the curve to calibrate light signals recorded from living cells. The correction should be far less important in the case of the obelins because the concentrations of Mg^{2+} likely to be found in living cells (around 1 mM) have very little effect on the position of the calcium concentration−effect curve.

Many different bioluminescent organisms are known or believed to contain Ca^{2+}-regulated photoproteins. Although apparently similar in their general mechanism of luminescence, these various photoproteins may differ in important ways, which will presumably come to light as more photoproteins are studied in detail. Such studies may reveal properties that are useful in themselves. However, even if they do not, the study of new photoproteins (especially together with their three-dimensional structures) may be expected to further our understanding of how bioluminescent proteins function and to provide clues to structure−activity relations. Such information may be exploited in the design of new artificial photoproteins that are already being created in the laboratory by means of site-directed mutagenesis.

ACKNOWLEDGMENT

We thank Michelle M. Herko for able technical assistance and Dr. Bruce Bryan for a gift of coelenterazine. One of us (J.L.) thanks the Whiteley Center, Friday Harbor Laboratories, for accommodation and use of facilities during the preparation of the manuscript.

REFERENCES

1. Shimomura, O., and Johnson, F. H. (1966) in *Bioluminescence in Progress* (Johnson, F. H., and Haneda, Y., Eds.) pp 496−521, Princeton University Press, Princeton, NJ.
2. Shimomura, O., and Johnson, F. H. (1975) *Nature 256*, 236−238.
3. Hastings, J. W., and Morin, J. G. (1969) *Biochem. Biophys. Res. Commun. 37*, 493−498.
4. Blinks, J. R. (1986) in *The Sarcoplasmic Reticulum in Muscle Physiology* (Entman, M. L., and Van Winkle, W. B., Eds.) Vol. II, pp 73−107, CRC Press, Boca Raton, FL.
5. Shimomura, O., Johnson, F. H., and Saiga, Y. (1962) *J. Cell. Comp. Physiol. 59*, 223−239.
6. Shimomura, O., and Johnson, F. H. (1972) *Biochemistry 11*, 1602−1608.
7. Cormier, M. J., Hori, K., Karkhanis, Y. D., Anderson, J. M., Wampler, J. E., Morin, J. G., and Hastings, J. W. (1973) *J. Cell. Physiol. 81*, 291−297.
8. Morin, J. G. (1974) in *Coelenterate Biology: Reviews and New Perspectives* (Muscatine, L., and Lenhoff, H. M., Eds.) pp 397−438, Academic Press, New York.
9. Shimomura, O., Saiga, Y., and Johnson, F. H. (1963) *J. Cell. Comp. Physiol. 62*, 9−15.
10. Levine, L. D., and Ward, W. W. (1982) *Comp. Biochem. Physiol. B72*, 77−85.
11. Campbell, A. K. (1974) *Biochem. J. 143*, 411−418.
12. Stephenson, D. G., and Sutherland, P. J. (1981) *Biochim. Biophys. Acta 678*, 65−75.
13. Bondar, V. S., Trofimov, K. P., and Vysotski, E. S. (1992) *Biokhimiya (Moscow) 57*, 1020−1027.
14. Ward, W. W., and Seliger, H. H. (1974) *Biochemistry 13*, 1491−1499.
15. Ward, W. W., and Seliger, H. H. (1974) *Biochemistry 13*, 1500−1510.
16. Prasher, D., McCann, R. O., and Cormier, M. J. (1985) *Biochem. Biophys. Res. Commun. 126*, 1259−1268.
17. Inouye, S., Noguchi, M., Sakaki, Y., Takagi, Y., Miyata, T., Iwanaga, S., Miyata, T., and Tsuji, F. I. (1985) *Proc. Natl. Acad. Sci. U.S.A. 82*, 3154−3158.
18. Prasher, D. C., McCann, R. O., Longiaru, M., and Cormier, M. J. (1987) *Biochemistry 26*, 1326−1332.

19. Inouye, S., and Tsuji, F. I. (1993) *FEBS Lett. 315*, 343−346.
20. Fagan, T. F., Ohmiya, Y., Blinks, J. R., Inouye, S., and Tsuji, F. I. (1993) *FEBS Lett. 333*, 301−305.
21. Illarionov, B. A., Markova, S. V., Bondar, V. S., Vysotski, E. S., and Gitelson, J. I. (1992) *Dokl. Akad. Nauk 326*, 911−913.
22. Illarionov, B. A., Bondar, V. S., Illarionova, V. A., and Vysotski, E. S. (1995) *Gene 153*, 273−274.
23. Charbonneau, H., Walsh, K. A., McCann, R. O., Prendergast, F. G., Cormier, M. J., and Vanaman, T. C. (1985) *Biochemistry 24*, 6762−6771.
24. Tsuji, F. I., Ohmiya, Y., Fagan, T. F., Toh, H., and Inouye, S. (1995) *Photochem. Photobiol. 62*, 657−661.
25. Head, J. F., Inouye, S., Teranishi, K., and Shimomura, O. (2000) *Nature 405*, 372−376.
26. Liu, Z.-J., Vysotski, E. S., Chen, C. J., Rose, J. P., Lee, J., and Wang, B. C. (2000) *Protein Sci. 9*, 2085−2093.
27. Vysotski, E. S., Liu, Z.-J., Deng, L., Rose, J. P., Lee, J., and Wang, B. C. (2001) in *Bioluminescence & Chemiluminescence 2000* (Case, J. F., Herring, P. J., Robison, B. H., Haddock, S. H. D., Kricka, L. J., and Stanley, P. E., Eds.) pp 135−138, World Scientific Publishing Co., Singapore.
28. Shimomura, O., and Johnson, F. H. (1978) *Proc. Natl. Acad. Sci. U.S.A. 75*, 2611−2615.
29. Blinks, J. R., Wier, W. G., Hess, P., and Prendergast, F. G. (1982) *Prog. Biophys. Mol. Biol. 40*, 1−114.
30. Hastings, J. W., Mitchell, G., Mattingly, P. H., Blinks, J. R., and van Leeuwen, M. (1969) *Nature 222*, 1047−1050.
31. Blinks, J. R., and Moore, E. D. W. (1986) in *Optical Methods in Cell Physiology* (De Weer, P., and Salzberg, B. M., Eds.) Vol. 40, pp 229−238. John Wiley, New York.
32. Illarionov, B. A., Frank, L. A., Illarionova, V. A., Bondar, V. S., Vysotski, E. S., and Blinks, J. R. (2000) *Methods Enzymol. 305*, 223−249.
33. Blinks, J. R., and Caplow, D. D. (1991) *Physiologist 34*, 110.
34. Shimomura, O., and Shimomura, A. (1985) *Biochem. J. 228*, 745−749.
35. Kendall, J. M., Sala-Newby, G., Ghalaut, V., Dormer, R. L., and Campbell, A. K. (1992) *Biochem. Biophys. Res. Commun. 187*, 1091−1097.
36. Chomczynski, P., and Sacchi, N. (1987) *Anal. Biochem. 162*, 156−159.
37. Blinks, J. R., Mattingly, P. H., Jewell, B. R., van Leeuwen, M., Harrer, G. C., and Allen, D. G. (1978) *Methods Enzymol. 57*, 292−328.
38. Klabusay, M., and Blinks, J. R. (1996) *Cell Calcium 20*, 227−234.
39. Blinks, J. R. (1989) *Methods Enzymol. 172*, 164−203.
40. Gibson, Q. H., and Milnes, L. (1964) *Biochem. J. 91*, 161−171.
41. Takagi, T., Konishi, K., and Cox, J. A. (1986) *Biochemistry 25*, 3585−3592.
42. Huang, B., Mengersen, A., and Lee, V. D. (1988) *J. Cell Biol. 107*, 133−140.
43. Marshak, D. R., Clarke, M., Roberts, D. M., and Watterson, D. M. (1984) *Biochemistry 23*, 2891−2899.
44. Wilkinson, J. M. (1976) *FEBS Lett. 70*, 254−256.
45. Jamieson, G. A., Jr., Bronson, D. D., Schachat, F. H., and Vanaman, T. C. (1980) *Ann. N.Y. Acad. Sci. 356*, 1−13.
46. Kumar, S., Harrylock, M., Walsh, K. A., Cormier, M. J., and Charbonneau, H. (1990) *FEBS Lett. 268*, 287−290.
47. Shimomura, O., and Johnson, F. H. (1969) *Biochemistry 8*, 3991−3997.
48. Morin, J. G., and Hastings, J. W. (1971) *J. Cell. Physiol. 77*, 305−311.
49. Shimomura, O., and Johnson, F. H. (1970) *Nature 227*, 1356−1357.
50. La, S. Y., and Shimomura, O. (1982) *FEBS Lett. 143*, 49−51.
51. Shimomura, O., and Teranishi, K. (2000) *Luminescence 15*, 51−58.
52. Lee, J., Glushka, J. N., Markova, S. V., and Vysotski, E. S. (2001) in *Bioluminescence & Chemiluminescence 2000* (Case, J. F., Herring, P. J., Robison, B. H., Haddock, S. H. D., Kricka, L. J., and Stanley, P. E., Eds.) pp 99−102, World Scientific Publishing Co., Singapore.
53. Zhang, W., Truttmann, A. C., Luethi, D., and McGuigan, J. A. S. (1997) *Anal. Biochem. 251*, 246−250.
54. Allen, D. G., Blinks, J. R., and Prendergast, F. G. (1977) *Science 195*, 996−998.

BI0117910